Transcriptomic analyses reveal the effects of grafting on anthocyanin biosynthesis in crabapple

Mengnan Zhao[1,2,3#], Sifan Wang[2,3#], Li Chen[3], Jie Zhang[2], Yuncong Yao[2,3*] (iD) and Ji Tian[2,3*]

[1] *College of Biological Sciences and Technology, Beijing Forestry University, Beijing 100083, China*
[2] *Beijing Advanced Innovation Center for Tree Breeding by Molecular Design, Beijing University of Agriculture, Beijing 102206, China*
[3] *Department of Plant Science and Technology, Beijing University of Agriculture, Beijing 102206, China*
[#] Authors contributed equally: Mengnan Zhao, Sifan Wang
[*] Corresponding authors, E-mail: yaoyc_20@126.com; tianji19850331@126.com

Abstract

Anthocyanins are crucial plant pigments that enhance plant color and bolster resistance. Grafting is an ancient cultivation technology in *Malus* production, and it has important effects on plant phenotypes, secondary metabolism, biotic, and abiotic resistance. However, the underlying genetic and regulatory mechanisms effects on anthocyanin biosynthesis are unclear. In this research, the phenotypic and transcriptome variation in *Malus* crabapple cv. 'Indian Magic' (Spring-red-leaf) and *Malus* Crabapple cv. 'Flame' (evergreen leaf) serving as either rootstock or scion (F/I, I/F) and self-grafted (I/I) as control were explored. The results showed that the anthocyanin accumulation in the stem of 'Flame' grafted onto 'Indian Magic' occurred rather than being induced by wounding and other stresses. Based on KEGG analyses, it was deduced that the anthocyanin accumulation is mainly induced by 'plant hormone signal transduction', 'starch and sucrose metabolism', and the 'MAPK signaling pathway'. Moreover, transcriptomic analyses also revealed *MdSAUR20* was highly induced during grafting, potentially playing a pivotal role in grafting-induced anthocyanin accumulation, as confirmed by transgenic assay. These results propose new insight into regulating anthocyanin biosynthesis and contributing signal transport in grafting, contributing to a better understanding of the selection and combination of scion and rootstock in the grafting process.

Introduction

Malus crabapple, a member of the Rosaceae family within the genus *Malus*, possesses an ornamental apple germplasm collection, representing an economically significant resource[1,2]. Commercial value in numerous ornamental plant species is strongly influenced by leaf color, and crabapple cultivars exhibit a diverse array of leaf colors. The variety of crabapple with red leaves has emerged as a significant breeding objective in recent years due to its high ornamental and landscaping value, which is widely appreciated by people.

Anthocyanins, members of the flavonoid family, play a role in imparting red coloration to crabapple leaves. The pathway for anthocyanin biosynthesis has been identified, including chalcone synthase (CHS), chalcone isomerase (CHI), flavanone 3-hydroxylase (F3H), dihydroflavonol 4-reductase (DFR), anthocyanidin synthase (ANS), UDP-glucose/flavonoid 3-O-glucosyltransferase (UFGT). Meanwhile, anthocyanin synthesis is also coordinated regulation by the MBW complex, consisting of MYB, basic helix-loop-helix proteins (bHLH), and WD40 proteins[3]. In apple, functional assays revealed *MdMYB1*, *MdMYB10*, and *MdMYBA* as crucial regulators of anthocyanin biosynthesis. This regulation occurs through their interaction with bHLH3 and WD40 proteins, activating the expression of genes involved in anthocyanin biosynthesis[4–6]. In land plants, anthocyanin biosynthesis is also induced by endogenous plant hormones[7]. Ethylene response factor gene (ERF), abscisic acid response factor gene (ABF), and jasmonic acid (JA) response

factor gene have been identified as activating the expression of anthocyanin biosynthetic genes, thus promoting anthocyanin accumulation[8–10]. Auxin and GA negatively regulate anthocyanin biosynthesis by triggering the degradation of auxin/indole-3-acetic acid (AUX/IAA) and DELLA proteins, respectively[11,12]. There were several major classes of auxin-responsive genes in plants that responded to changes in auxin levels, including the Auxin/Indole-3-Acetic Acid (Aux/IAA) family, the auxin response factor (ARF) family, small auxin upregulated RNA (SAUR), and the auxin-responsive Gretchen Hagen3 (GH3) family[13]. Among these SAURs are the most rapid auxin-responsive genes related to the auxin signaling pathway[14]. Then, the gene function of the SAURs family have been identified in various plants, *AtSAUR19–24* were verified as positive regulators of plant cell expansion[15]. *MdSAUR36* was confirmed to participate in the negative regulation of mesocarp cell division and fruit size in *Malus* species[16]. However, the function of anthocyanin synthesis of SAUR family members still needs further study.

Grafting in plants, a conventional technique for asexual propagation typically involves joining two plant segments. It serves to propagate consistent seedlings of several valuable fruit species, enhance disease and stress resistance, and prevent a juvenile state. This method is extensively applied in modern horticultural production, including crops like apple, citrus, pear, grape, kiwifruit, and lychee[17–20].

Grafting involves the physical connection of separate plant parts, where rootstock and scion share an interconnected

vascular system. Within this system, several small peptides, proteins and RNA molecules have been identified as mobile in xylem or phloem, capable of triggering physiological variations through the graft junction, leading to enhanced vigor[21−23]. Studies involving apple genotypes have demonstrated that oligopeptide transporter 3 (*MdOPT3*) mRNA can traverse long distances, from the leaf to the root, regulating iron uptake[24]. Furthermore, *MdCAX3* mRNA has been observed to move from leaves to roots, contributing to the control of iron and zinc homeostasis under iron-starvation conditions[25]. Recent researchers have also demonstrated that secondary metabolites can be promoted by grafting with rootstocks in plants. For instance, in grapevines, heterografting enhances the accumulation of flavonoids in grape berry skin during development, accompanied by an increase in the transcription of related biosynthesis genes[26]. However, there is limited available data concerning the impact of different rootstocks on the dynamic changes in anthocyanin accumulation in crabapple leaves.

In this study, the focus was on investigating the impact of diverse scion-rootstock combinations on physiological parameters and gene transcription in crabapple leaves. *Malus* crabapple cv. 'Indian Magic' (Spring-red-leaf) and *Malus* Crabapple cv. 'Flame' (evergreen leaf) were employed as either rootstock or scion (F/I, I/F), and self-grafted (I/I) served as the control. The aim was to identify key anthocyanin regulatory genes through RNA-seq analysis. The results demonstrated a significant accumulation of anthocyanin in the stem of 'Flame' within the I/F combination, with *MdSAUR20* identified as a candidate regulator during the grafting process. The present investigation contributes to an enhanced understanding of the selection and combination of scion and rootstock in the grafting process, providing valuable insights for *Malus* breeding.

Materials and methods

Plant materials and grafting

Malus crabapple cv. 'Flame' (evergreen leaf) and *Malus* crabapple cv. 'Indian Magic' (Spring-red-leaf) were selected for this experiment. Before grafting, *Malus* plants were grown in Murashig and Skoog (MS) medium for 1 month. The grafted plants were used for phenotypic observation and sampling for RNA-seq. Grafting of crabapple was performed using an insect pin into the scion as previously described[27]. Grafting combinations were as follows: 'Flame' as scion and 'Indian Magic' as rootstock (F/I), 'Indian Magic' as scion and 'Flame' as rootstock (I/F); self-grafted 'Flame'/'Flame' (F/F) and 'Indian Magic'/'Indian Magi' (I/I) were used as control[28−30].

RNA extraction, sequencing, and Differentially Expressed Genes (DEGs) identification

Total RNA was extracted from the stem of scions and rootstocks and seedling samples using an RNA Extraction Kit (Vazyme, Nanjing, China) according to the manufacturer's instructions. Further, RNA-seq libraries were constructed and sequenced on NovaSeq platform. Hisat2 v2.0.5 was used to align clean reads to the apple genome. Featuretsv1.5.0-p3 was used to map read numbers to each gene. Differential expression analysis was performed using the DESeq2 R package (1.16.1)[31]. KEGG (Kyoto Encyclopedia of Genes and Genomes) pathways were tested by KOBAS software[32].

Measurement of anthocyanin content

Frozen stem of *Malus* crabapple and seedlings samples (0.1 g fresh weight) were ground in 1 mL extraction buffer (methanol:formic acid:water = 80:1:19). The pH-differential method to measure the total content anthocyanin was carried out as referenced by Salas et al.[33]. Total anthocyanin contents were quantified spectrophotometrically at 530 and 700 nm as previously described[34].

Gene cloning and transient transformation of apple tissue culture seedlings

'Red Fuji' apple peel cDNA was used as a template to clone the full-length of *MdSAUR20* (MD05G1052200) (primer information is listed in Supplemental Table S1). The *MdSAUR20* coding sequence was cloned into the pRI101-eGFP vector for gene overexpression of apple tissue culture seedlings (*M. domestica* cv. 'Golden Delicious') were grown in a subculture medium (MS +1 mg/L 6-BA + 0.2 mg/L NAA + 0.5 mg/L GA) under long-day conditions (16-h light/8-h darkness, 24 °C). Transgenic seedlings were obtained by *Agrobacterium*-mediated transformation and vacuum extraction. For detailed transient methods refer to the previous study by Liu et al.[35].

RT-qPCR analysis

Quantitative real-time PCR analysis was proceeded with SYBR Green qPCR kit (Vazyme, Nanjing, China) according to the manufacturer's instructions. The data were analyzed using the internal control and the $2^{−\Delta\Delta C_T}$ method[36]. Primer sequences are listed in Supplemental Table S1.

Results

Anthocyanin accumulation of scions were affected by rootstocks in grafting

To examine the impact of rootstock on scion anthocyanin accumulation during grafting, various scion-rootstock combinations were generated. The results revealed significant anthocyanin accumulation in the stem in the F/I combination, indicating the influence of rootstock on scion pigmentation. In Fig. 1a, when the spring red cultivar 'Indian Magic' served as the rootstock, the green stem of the evergreen cultivar 'Flame' turned red. Meanwhile, there was also anthocyanin accumulation in the stem of 'Indian Magic' when 'Flame' was used as rootstock. To distinguish whether anthocyanin accumulation in the stem of 'Flame' resulted from grafting rather than other stresses, we used F/F and I/I combinations as controls. Anthocyanin was not detected in the stem of 'Flame' when 'Flame' was used as rootstock, and the stem of 'Indian Magic' maintained a red color when 'Indian Magic' was used as rootstock. The results confirmed that the 'Indian Magic' rootstock promoted anthocyanin accumulation in the stem of the 'Flame' scion. Paraffin sections were conducted to observe the stem's cross-section, revealing a hollow in the vascular system, indicating a vascular connection between the rootstock and scion in F/I (Fig. 1b). In summary, the use of an anthocyanin-rich cultivar as rootstock may influence anthocyanin accumulation through signaling mechanisms during grafting.

Overview of the transcriptomic data between grafting combinations

To gain an in-depth comprehension of the regulatory mechanism of anthocyanin accumulation during grafting, the stems
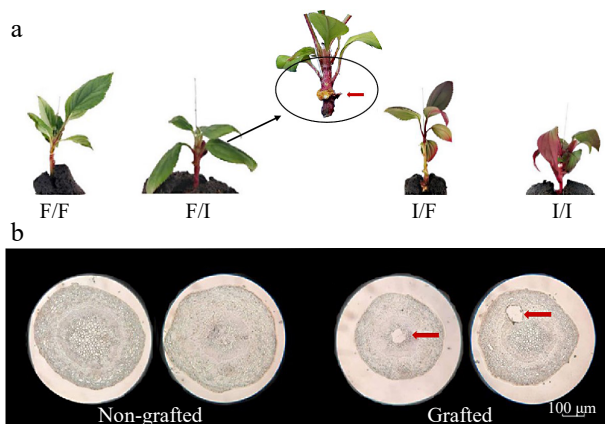
Fig. 1 Grafting affects anthocyanin accumulation in F/I combination. (a) Phenotype of grafted seedlings with differential grafting combinations (red arrows indicate the bonding sites of scion and rootstock, the black circle is the anthocyanin accumulation area) (F/F: *Malus* crabapple cv. 'Flame' as scion and *Malus* crabapple cv. 'Flame' as rootstock; F/I: *Malus* crabapple cv. 'Flame' as scion and *Malus* crabapple cv. 'Indian Magic' as rootstock; I/F: *Malus* crabapple cv. 'Indian Magic' as scion and *Malus* crabapple cv. 'Flame' as rootstock; I/I: *Malus* crabapple cv. 'Indian Magic' as scion and rootstock). (b) Paraffin section of the interface in non-grafted and grafted seedlings.

Table 1. RNA sequencing data.

Sample name	Clean reads	% ≥ Q30	Total reads	Mapped reads
I-I-R-1	26,367,340	93.26	52,734,680	45,507,642 (86.3%)
I-I-R-2	22,928,739	93.21	45,857,478	39,118,647 (85.3%)
I-I-R-3	22,104,191	93.99	44,208,382	38,710,947 (87.56%)
I-I-S-1	23,790,350	93.89	47,580,700	41,410,502 (87.03%)
I-I-S-2	23,041,216	93.29	46,082,432	40,172,269 (87.17%)
I-I-S-3	23,120,817	93.00	46,241,634	40,433,561 (87.44%)
I-F-S-1	23,048,140	94.00	46,096,280	40,314,380 (87.46%)
I-F-S-2	22,692,497	93.90	45,384,994	40,033,821 (88.21%)
I-F-S-3	19,344,387	93.00	38,688,774	33,125,491 (85.62%)
I-F-R-1	22,931,226	94.37	45,862,452	40,818,713 (89.0%)
I-F-R-2	22,311,552	93.06	44,623,104	38,436,230 (86.14%)
I-F-R-3	22,713,776	93.84	45,427,552	39,092,461 (86.05%)
F-I-S-1	22,724,018	94.15	45,448,036	40,037,863 (88.1%)
F-I-S-2	23,260,096	93.93	46,520,192	39,871,870 (85.71%)
F-I-S-3	22,846,841	94.05	45,693,682	40,535,794 (88.71%)
F-I-R-1	23,151,622	94.06	46,303,244	41,035,064 (88.62%)
F-I-R-2	25,981,536	94.19	51,963,072	45,465,386 (87.5%)
F-I-R-3	23,629,467	94.19	47,258,934	41,551,698 (87.92%)

Clean reads: number of reads after raw data filtering; % ≥ Q30: Percentage of total bases with Phred values greater than 30; Total reads: number of clean reads of sequencing data after quality control; Mapped reads: number of reads matched to the genome and their percentages.

of scions (-S) and rootstocks (-R) in F/I, I/F, I/I combinations were used as materials for transcriptome sequencing. Three biological replicates for each combination were investigated, and clean reads ranged from 38,688,774 to 52,734,680, between 85.3% to 88.71% of the sequenced reads aligned with the apple reference genome. All 18 libraries exhibited Q30 percentages surpassing 93% (Table 1). Pearson correlation analysis and principle component analysis demonstrated highly correlated transcriptome characteristics among the biological replicates in differential grafting combinations ($R^2 = 0.747 − 0.962$) (Fig. 2a). A principle component analysis also indicated that F-I-S and I-F-R were more separated from other samples (Fig. 2b). These findings suggest that the main differences induced by grafting occur in the scion of 'F/I' and the rootstock of 'I-F'.

Identification of genes showing differential expression during grafting

To detect differentially expressed genes in scion and rootstock across F/I, I/F, I/I combinations, comparisons were conducted as follows: F-I-S vs I-F-R, F-I-R vs I-I-R, and I-F-S vs I-I-S, and the sequenced genes were filtered using $|log_2(foldchange)| > 0$ and rate (FDR) < 0.05 as the screening criteria. In F-I-S vs I-F-R, 145 DEGs were found that met the filtering criteria, comprising 85 up-regulated and 60 down-regulated DEGs (Fig. 3a). For F-I-R vs I-I-R, 205 DEGs were filtered, comprising 188 up-regulated and 17 down-regulated DEGs (Fig. 3b). In I-F-S vs I-I-S, 747 DEGs were filtered, with 433 DEGs up-regulated and 314 DEGs down-regulated (Fig. 3c). The maximum number of DEGs in I-F-S vs I-I-S suggests that grafting in different rootstocks results in significant differential gene expression.

To elucidate the clustering pattern of DEGs, KEGG analyses was conducted for the three grafting combinations: F-I-S vs I-F-R, F-I-S vs I-I-R, and I-F-S vs I-I-S. KEGG analysis aimed to discern the biological functions of the identified DEGs through pairwise comparisons. Compared F-I-S with I-F-R, these DEGs were

with enrichment in the following pathways: 'Plant hormone signal transduction', 'Starch and sucrose metabolism', 'MAPK signaling pathway', 'Arginine and proline metabolism', 'Diterpenoid biosynthesis' (Fig. 4a). F-I-R in contrast to I-I-R, the results confirmed that DEGs were enrichment in the following pathways: 'Amino sugar and nucleotide sugar metabolism', 'Plant pathogen interaction', 'MAPK signaling pathway', 'Plant hormone signal transduction' (Fig. 4b). Moreover, comparing I-F-S with I-I-S, the results suggested that the DEGs were enriched in the 'ribosome', 'carbon metabolism' 'starch and sucrose metabolism', 'phenylpropanoid biosynthesis', 'amino sugar and nucleotide sugar metabolism' (Fig. 4c). According to the KEGG analyses, it was deduced that the accumulation of anthocyanin was mainly mediated by 'plant hormone signal transduction', 'Starch and sucrose metabolism', 'MAPK signaling pathway', 'arginine and proline metabolism'. Meanwhile, Auxin related genes auxin-induced protein AUX28, SAUR32-like, IAA3-like, and gibberellin receptor GID1B-like were identified in the 'Plant hormone signal transduction' pathway, which suggested that auxin and GA may have important roles in the grafting process (Supplemental Table S2). To understand the biological processes involved in grafting in different combinations, Gene Ontology (GO) analysis was performed. DEGs in the 'cell periphery', 'external encapsulating structure' and 'cell wall' terms were significantly enriched in F-I-S vs I-F-R. In F-I-R vs I-I-R, the DEGs were enriched in the 'cell periphery', 'extracellular region', and 'calcium ion binding' terms. Comparing I-F-S vs I-I-S, these DEGs were enriched in the 'intracellular non-membrane bounded organelle', 'non-membrane bounded organelle', 'ribonucleoprotein complex', and 'ribosome' terms.

Identification of genes associated with anthocyanin biosynthesis during grafting

To identify key anthocyanin regulators during grafting in crabapple, we focused on DEGs that met the criteria $|log_2(foldchange)| > 2$ and false discovery rate (FDR) < 0.05 between different combinations. In the comparison of F-I-S vs I-F-R, there
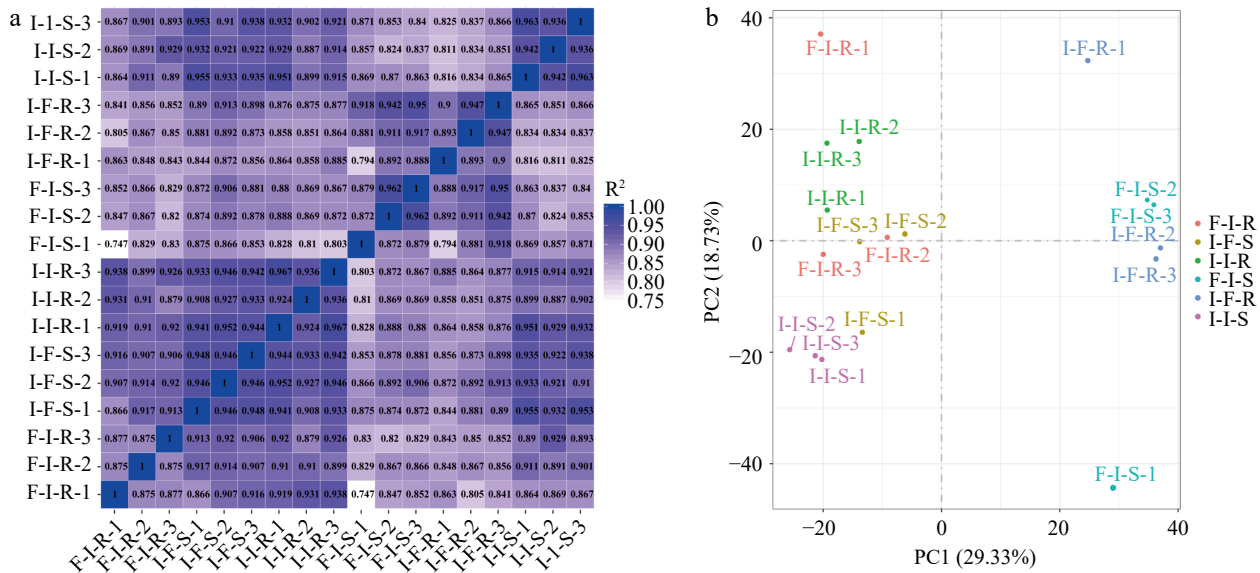
Fig. 2 Transcriptome analyses of stem of scions and rootstock in different grafting combinations. (a) Pearson correlation between samples (the horizontal and vertical coordinates of the graph are the square of the correlation coefficient of each sample). (b) Principal component analysis of samples.
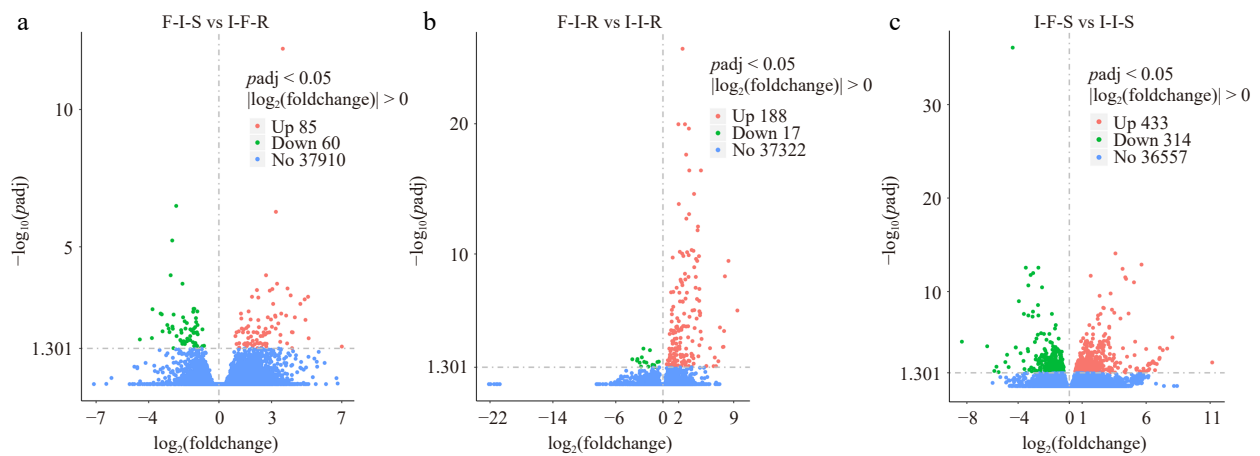

Fig. 3 The number of differential expressed genes for compare group. The horizontal coordinate is the $\log_2$(foldchange) value, the vertical coordinate is $-\log_{10}$($p$adj) or $-\log_{10}$($p$value), and the threshold line for the differential gene screening criteria.

were 120 DEGs listed in Supplemental Table S3. Among them, three transcription factors *MdSAUR20-like* (MD05G1052200), *MdbHLH137* (MD06G1133200), *MdbHLH63-like* (MD05G1065100) were identified and the variation of expression level of these three TFs in the comparison. Notably, *MdSAUR20* showed the highest expression in F-I-S. The expression level of *MdSAUR20* was also analyzed by qRT-PCR, and the results showed that *MdSAUR20* in the stem of 'Flame' in F-I-S was significantly higher than that in the stem of 'Indian Magic' I-F-S, suggesting its potential role as a key signaling factor for anthocyanin accumulation in the scion during the grafting process (Fig. 5b).

To unravel the transcriptional regulatory mechanism of *MdSAUR20*, *cis*-elements in the promoter region of *MdSAUR20* were examined using the PlantCARE database. The analysis identified the presence of TGACG, CGTCA-motif, ABRE, and TCA motifs in the *MdSAUR20* promoter. From this, it can be inferred that the expression of *MdSAUR20* could potentially be triggered by Indole acetic acid (IAA), Methyl Jasmonate (MeJA), Abscisic acid (ABA) and Salicylic acid (SA) (Fig. 5d).

To further investigate the role of *MdSAUR20* in anthocyanin biosynthesis, overexpression assays were conducted in apple tissue culture seedlings (*M. domestica* cv. 'Golden Delicious') using the vector pRI101-eGFP vector. The seedling transformed with pRI101-*MdSAUR20*-eGFP exhibited a noticeable color difference compared to the control (Fig. 6a). Measurement of anthocyanin analysis further confirmed an increase in anthocyanin accumulation in the *MdSAUR20* overexpressed seedling (Fig. 6b). qRT-PCR results demonstrated significantly elevated transcription levels of anthocyanin biosynthesis genes, including *MdCHS*, *MdCHI*, *MdF3H*, *MdDFR*, *MdANS* and *MdUFGT* genes, in the *MdSAUR20* overexpressed seedling compared to the control (Fig. 6c).

Discussion

Grafting stands as a crucial agricultural method, elevating the vigor and characteristics of the scion, impacting various aspects such as fruit quality, fruit color, environmental and
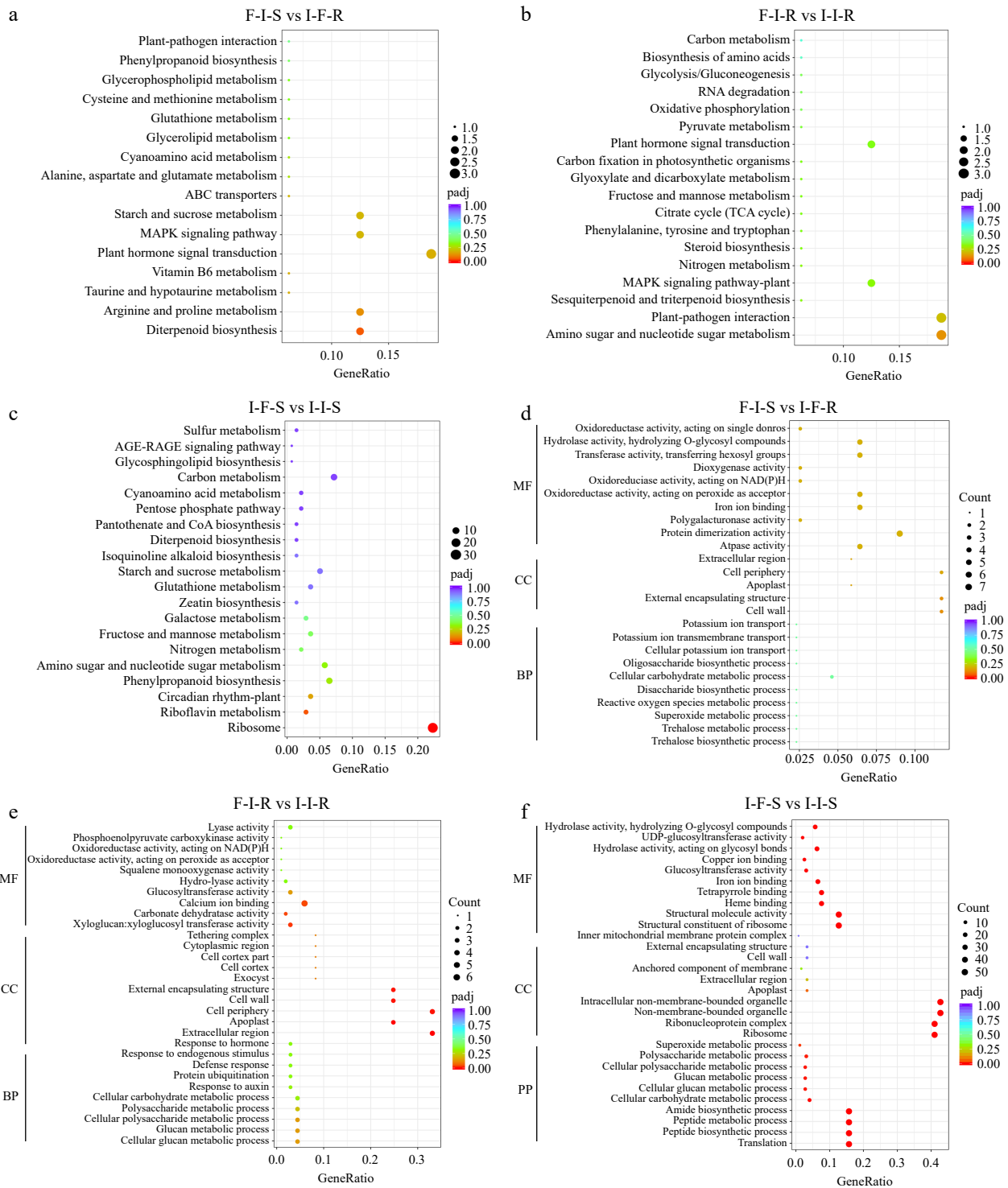
Fig. 4 Functional analysis of differentially expressed genes between grafting combinations. (a) KEGG enrich analyses in F-I-S vs I-F-R, (b) KEGG enrich analyses in F-I-R vs I-I-R, (c) KEGG enrich analyses in I-F-S vs I-I-S, (d) GO enrich analyses in F-I-S vs I-F-R, (e) GO enrich analyses in F-I-R vs I-I-R, (f) GO enrich analyses in I-F-S vs I-I-S.

disease stress resistance[37]. Anthocyanins, the primary pigments in *Malus* plants, assume vital functions in multiple physiological and biochemical processes, encompassing UV protection, insect attraction, herbivore defense[38–40]. Therefore, the utilization of cultivars with elevated anthocyanin content as rootstocks have significant production importance.

However, the molecular regulatory mechanisms governing anthocyanin biosynthesis during grafting in *Malus* plants remain unclear. In the present study, the evergreen cultivar 'Flame' and the spring-red-leaf cultivar 'Indian Magic' were selected as grafting materials. The results revealed that the accumulation of anthocyanin was induced in the 'Flame' when
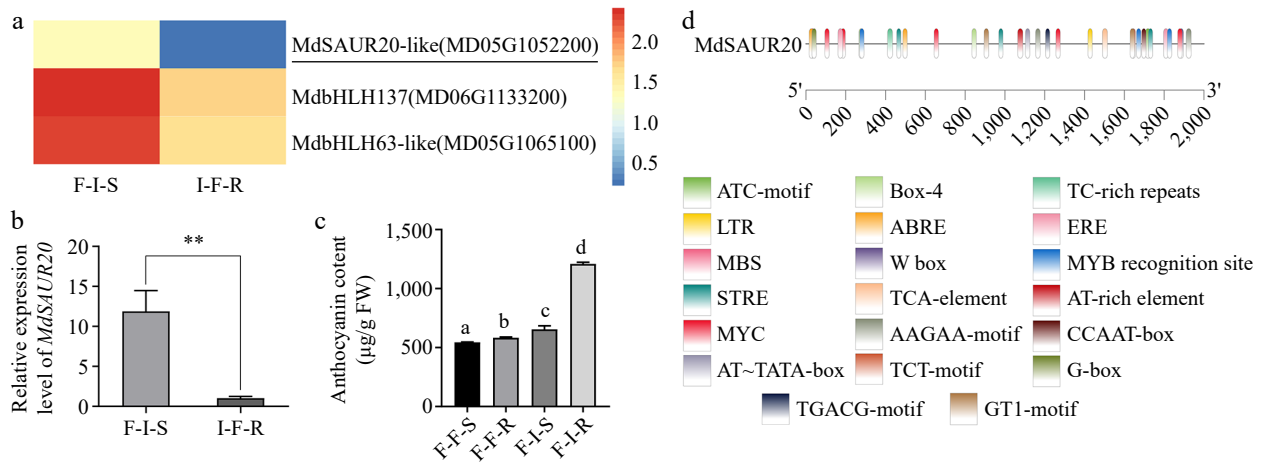
Fig. 5 Analysis of genes associated with anthocyanin biosynthesis during grafting. (a) Heatmap describing the expression of candidate transcription factors. (b) Relative expression levels of *MdSAUR20* in F-I-S and I-F-R. (c) The content of anthocyanin in F/F vs F/I. (d) Schematic diagrams of the *MdSAUR20* promoters. The error bars indicate the SD of three biological replicates. Asterisks indicate statistically significant differences (*$p < 0.05$; **$p < 0.01$) according to Student's t test.
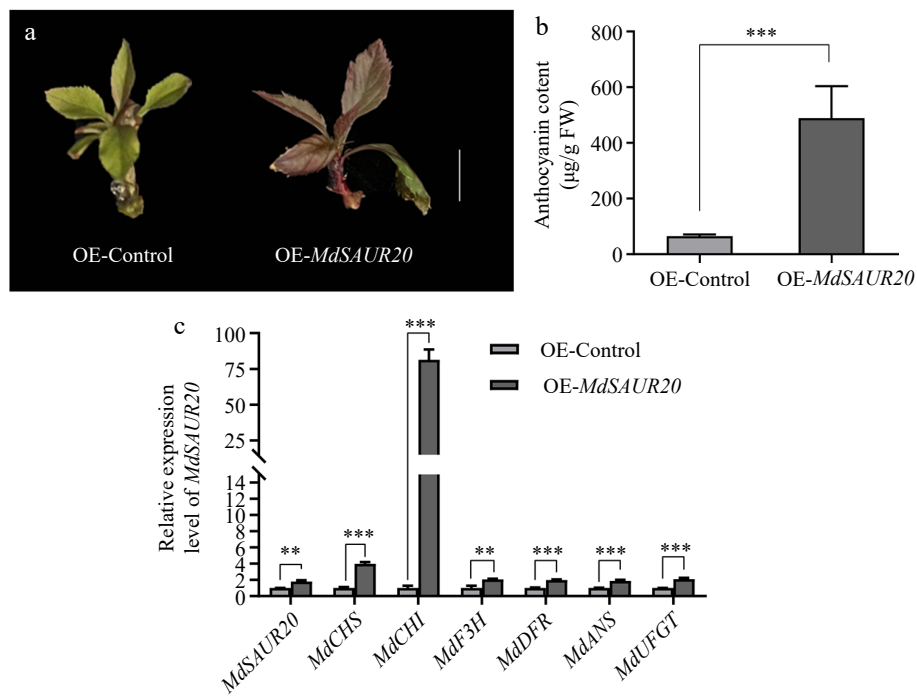

Fig. 6 Functional assay of in *MdSAUR20*. (a) Pigmented transgenic cells were formed in seedling transformed with OE-*MdSAUR20*. Scale bar = 1 cm (b) Anthocyanin content in inoculated apple tissue culture seedlings. (c) Relative expression levels of *MdSAUR20* in seedlings and anthocyanin biosynthesis genes. Data are presented as mean values ± SD of three independent biological replicates. Asterisks indicate significant difference by Student's t-test.

'Indian Magic' was used as the rootstock. Furthermore, through RNA-seq analysis, *MdSAUR20* was identified as a crucial regulator of anthocyanin during grafting.

Grafting can modify scion phenotypes through the uptake and transport of water, nutrients, hormones, and long-distance movement of biological molecules[37]. Micrografting experiments in *Arabidopsis*, employing different mutants related to cytokinin biosynthesis and transport demonstrated that the regulation of shoot architecture is influenced by the root-to-shoot translocation of trans-zeatin riboside and trans-zeatin[41]. In blood oranges, eight developmental stages of the lido blood

orange cultivar grafted onto two rootstocks, and global transcriptome and metabolome results revealed that flavonoid-accumulating rootstocks predominantly influence the fruit quality of the scion[37]. In grape, the metabolomic analysis of *Cabernet Sauvignon* cultivar grafted onto different rootstocks and onto itself demonstrated that grafting promotes the accumulation of stilbenes, anthocyanins, PAs, and flavonols[41,42]. Phenotypic, metabolomic, and transcriptomic results also indicated that grafting the Crimson Seedless cultivar onto four rootstocks could enhance berry color[37]. These results suggest that various rootstocks have the potential ability to improve

anthocyanin accumulation in fruit through grafting. However, the molecular mechanism and signal transport mode remain unclear. In the present results, it was observed that 'Indian Magic' rootstock promoted anthocyanin accumulation in the stem of 'Flame' scion. KEGG analysis further suggested that anthocyanin accumulation in the scions of 'Flame' grafted onto 'Indian Magic' rootstock may be mediated by plant hormones, starch, and sucrose, or other signal transduction pathways. We speculate that variations in anthocyanin accumulation during grafting depend on differentially expressed genes and the transmission of multiple signaling pathways.

Plant hormones are likely to be important factors that modulate light-dependent anthocyanin accumulation. Previous investigations have demonstrated the existence of crosstalk between hormone signaling pathways and anthocyanin biosynthetic pathway, IAA enhanced the cytokinin-induced increase in anthocyanin levels in *Arabidopsis* and *M. domastic* cv. 'Red Delicious'[43,44]. In apple, auxin response factor MdARF13 negatively regulates anthocyanin biosynthesis by interacting with MdMYB10 and MdIAA121 interacts with MdARF13 to weaken the inhibition of anthocyanin biosynthesis[11]. And other studies found that the E3 ubiquitin ligases MdSINA4 and MdSINA11 were involved in auxin-mediated anthocyanin regulation by triggering the ubiquitination degradation of MdIAA29 and MdARF5 which auxin suggested plays a key role in mediating the inhibition of anthocyanin biosynthesis[45]. In conclusion, the identification of DEGs between F-I-S and I-F-R suggests that *MdSAUR20* (MD05G1052200) may be induced by plant hormones and serves as a regulator of anthocyanin biosynthesis during grafting.

Conclusions

In summary, the comprehensive phenotypic and transcriptomic analyses during grafting have provided valuable insights into anthocyanin synthesis. These findings reveal noteworthy alterations in transcriptional patterns related to color regulation under diverse grafting conditions, presenting implications for the improvement and breeding of *Malus* plants.

Author contributions

The authors confirm contribution to the paper as follows: experiments design: Tian J, Yao Y; experiments performing: Zhao M, Wang S, Chen L; data analysis: Zhao M, Wang S, Zhang J; reagents/materials contributing: Tian J, Yao Y; manuscript writing: Zhao M, Wang S. All authors reviewed the results and approved the final version of the manuscript.

Data availability

RNA-sequencing data in this study have been deposited in the NCBI Bioproject database under accession number (PRJNA1066043, https://dataview.ncbi.nlm.nih.gov/object/PRJNA1066043).

Acknowledgments

Conflict of interest

The authors declare that they have no conflict of interest.

Supplementary Information accompanies this paper at (https://www.maxapress.com/article/doi/10.48130/opr-0024-0018)

Dates

References

1. Tian J, Peng Z, Zhang J, Song T, Wan H, et al. 2015. *McMYB10* regulates coloration via activating *McF3'H* and later structural genes in ever-red leaf crabapple. *Plant Biotechnology Journal* 13:948−61
2. Tai D, Tian J, Zhang J, Song T, Yao Y. 2014. A *Malus* crabapple chalcone synthase gene, *McCHS*, regulates red petal color and flavonoid biosynthesis. *PLoS One* 9:e110570
3. Saito K, Yonekura-Sakakibara K, Nakabayashi R, Higashi Y, Yamazaki M, et al. 2013. The flavonoid biosynthetic pathway in *Arabidopsis*: structural and genetic diversity. *Plant Physiology Biochemistry* 72:21−34
4. Ban Y, Honda C, Hatsuyama Y, Igarashi M, Bessho H, et al. 2007. Isolation and functional analysis of a MYB transcription factor gene that is a key regulator for the development of red coloration in apple skin. *Plant Cell Physiology* 48:958−70
5. Espley RV, Hellens RP, Putterill J, Stevenson DE, Kutty-Amma S, et al. 2007. Red colouration in apple fruit is due to the activity of the MYB transcription factor, *MdMYB10*. *The Plant Journal* 49:414−27
6. Takos AM, Jaffé FW, Jacob SR, Bogs J, Robinson SP, et al. 2006. Light-induced expression of a *MYB* gene regulates anthocyanin biosynthesis in red apples. *Plant Physiology* 142:1216−32
7. Yang T, Ma H, Li Y, Zhang Y, Zhang J, et al. 2021. Apple MPK4 mediates phosphorylation of MYB1 to enhance light-induced anthocyanin accumulation. *The Plant Journal* 106:1728−45
8. Wang S, Li L L, Zhang Z, Fang Y, Li D, Chen X et al. 2022. Ethylene precisely regulates anthocyanin synthesis in apple via a module comprising MdEIL1, MdMYB1, and MdMYB17. *Horticulture Research* 9:uhac034
9. An J, Zhang X, Liu Y, Wang X, You C, et al. 2021. ABI5 regulates ABA-induced anthocyanin biosynthesis by modulating the *MYB1-bHLH3* complex in apple. *Journal of Experimental Botany* 72:1460−72
10. Qi T, Song S, Ren Q, Wu D, Huang H, Chen Y, et al. 2011. The Jasmonate-ZIM-domain proteins interact with the WD-repeat/bHLH/MYB complexes to regulate jasmonate-mediated anthocyanin accumulation and trichome initiation in *Arabidopsis thaliana*. *The Plant Cell* 23:1795−814
11. Wang Y, Wang N, Xu H, Jiang S, Fang H, et al. 2018. Auxin regulates anthocyanin biosynthesis through the Aux/IAA-ARF signaling pathway in apple. *Horticulture Research* 5:59
12. Xie Y, Tan H, Ma Z, Huang J. 2016. DELLA proteins promote anthocyanin biosynthesis via sequestering *MYBL2* and JAZ suppressors of the MYB/bHLH/WD40 complex in *Arabidopsis thaliana*. *Molecular Plant* 9:711−21
13. Luo J, Zhou J, Zhang J. 2018. *Aux/IAA* gene family in plants: molecular structure, regulation, and function. *International Journal of Molecular Sciences* 19:259

14. Wang P, Lu S, Xie M, Wu M, Ding S, et al. 2020. Identification and expression analysis of the small auxin-up RNA (SAUR) gene family in apple by inducing of auxin. *Gene* 750:144725

15. Spartz AK, Lee SH, Wenger JP, Gonzalez N, Itoh H, et al. 2012. The *SAUR19* subfamily of SMALL AUXIN UP RNA genes promote cell expansion. *The Plant Journal* 70:978−90

16. Tian Z, Wu B, Liu J, Zhang L, Wu T, et al. 2024. Genetic variations in *MdSAUR36* participate in the negative regulation of mesocarp cell division and fruit size in *Malus species*. *Molecular Breeding* 44:1

17. Yang Y, Huang M, Qi L, Song J, Li Q, et al. 2017. Differential expression analysis of genes related to graft union healing in *Pyrus ussuriensis* Maxim by cDNA-AFLP. *Scientia Horticulturae* 225:700−06

18. Li D, Han F, Liu X, Lv H, Li L, et al. 2021. Localized graft incompatibility in kiwifruit: analysis of homografts and heterografts with different rootstock & scion combinations. *Scientia Horticulturae* 283:110080

19. Chen Z, Zhao J, Hu F, Qin Y, Wang X, et al. 2017. Transcriptome changes between compatible and incompatible graft combination of *Litchi chinensis* by digital gene expression profile. *Scientific Reports* 7:3954

20. Melnyk CW, Meyerowitz EM. 2015. Plant grafting. *Current Biology* 25:R183−R188

21. Li H, Testerink C, Zhang Y. 2021. How roots and shoots communicate through stressful times. *Trends in Plant Science* 26:940−52

22. Duan X, Zhang W, Huang J, Hao L, Wang S, et al. 2016. *PbWoxT1* mRNA from pear (*Pyrus betulaefolia*) undergoes long-distance transport assisted by a polypyrimidine tract binding protein. *New Phytologist* 210:511−24

23. Kurotani KI, Notaguchi M. 2021. Cell-to-cell connection in plant grafting-molecular insights into symplasmic reconstruction. *Plant and Cell Physiology* 62:1362−71

24. Lv X, Sun Y, Hao P, Zhang C, Tian J, et al. 2021. RBP differentiation contributes to selective transmissibility of *OPT3* mRNAs. *Plant Physiology* 187:1587−604

25. Hao P, Lv X, Fu M, Xu Z, Tian J, et al. 2022. Long-distance mobile mRNA *CAX3* modulates iron uptake and zinc compartmentalization. *EMBO Reports* 23:e53698

26. Zhang F, Zhong H, Zhou X, Pan M, Xu J, et al. 2022. Grafting with rootstocks promotes phenolic compound accumulation in grape berry skin during development based on integrative multi-omics analysis. *Horticulture Research* 9:uhac055

27. Huang N, Yu T. 2021. Non-sterile grafting methods for *Arabidopsis*. In *Arabidopsis Protocols*, Sanchez-Serrano JJ, Salinas J. Humana, New York, NY. 2200:113−19. https://doi.org/10.1007/978-1-0716-0880-7_4

28. Zhang J, Xu H, Wang N, Jiang S, Fang H, et al. 2018. The ethylene response factor *MdERF1B* regulates anthocyanin and proanthocyanidin biosynthesis in apple. *Plant Molecular Biology* 98:205−18

29. An J, Zhang X, You C, Bi S, Wang X, et al. 2019. *MdWRKY40* promotes wounding-induced anthocyanin biosynthesis in association with *MdMYB1* and undergoes MdBT2-mediated degradation. *New Phytologist* 224:380−95

30. An J, Wang X, Zhang X, Xu H, Bi S, et al. 2020. An apple MYB transcription factor regulates cold tolerance and anthocyanin accumulation and undergoes MIEL1-mediated degradation. *Plant Biotechnology Journal* 18:337−53

31. Love MI, Huber W, Anders S. 2014. Moderated estimation of fold change and dispersion for RNA-seq data with DESeq2. *Genome Biology* 15:550

32. Kanehisa M, Goto S. 2000. KEGG: kyoto encyclopedia of genes and genomes. *Nucleic Acids Research* 28:27−30

33. Salas E, Dueñas M, Schwarz M, Winterhalter P, Cheynier V, et al. 2005. Characterization of pigments from different high speed countercurrent chromatography wine fractions. *Journal of Agricultural and Food Chemistry* 53:4536−46

34. Wang S, Li L, Fang Y, Li D, Mao Z, et al. 2022. MdERF1B-MdMYC2 module integrates ethylene and jasmonic acid to regulate the biosynthesis of anthocyanin in apple. *Horticulture Research* 9:uhac142

35. Liu Y, Zhang X, Liu X, Zheng P, Su L, et al. 2022. Phytochrome interacting factor MdPIF7 modulates anthocyanin biosynthesis and hypocotyl growth in apple. *Plant Physiology* 188:2342−63

36. Livak KJ, Schmittgen TD. 2001. Analysis of relative gene expression data using real-time quantitative PCR and the $2^{-\Delta\Delta C_T}$ method. *Methods* 25:402−08

37. Zhong H, Liu Z, Zhang F, Zhou X, Sun X, et al. 2022. Metabolomic and transcriptomic analyses reveal the effects of self- and heterografting on anthocyanin biosynthesis in grapevine. *Horticulture Research* 9:uhac103

38. Holton TA, Cornish EC. 1995. Genetics and biochemistry of anthocyanin biosynthesis. *The Plant Cell* 7:1071−83

39. Winkel-Shirley B. 2001. Flavonoid biosynthesis. A colorful model for genetics, biochemistry, cell biology, and biotechnology. *Plant Physiology* 126:485−93

40. Andersen OM, Markham KR. 2006. *Flavonoids. Chemistry, biochemistry and application*. Boca Raton: CRC Press. 1256 pp. https://doi.org/10.1201/9781420039443

41. Osugi A, Kojima M, Takebayashi Y, Ueda N, Kiba T, et al. 2017. Systemic transport of *trans*-zeatin and its precursor have differing roles in *Arabidopsis* shoots. *Nature Plants* 3:17112

42. Wang Y, Chen W, Gao X, He L, Yang X, et al. 2019. Rootstock-mediated effects on *cabernet sauvignon* performance: vine growth, berry ripening, flavonoids, and aromatic profiles. *International Journal of Molecular Sciences* 20:401

43. Li W, Mao J, Yang S, Guo Z, Ma Z, et al. 2018. Anthocyanin accumulation correlates with hormones in the fruit skin of 'Red Delicious' and its four generation bud sport mutants. *BMC Plant Biology* 18:363

44. Loreti E, Povero G, Novi G, Solfanelli C, Alpi A, et al. 2008. Gibberellins, jasmonate and abscisic acid modulate the sucrose-induced expression of anthocyanin biosynthetic genes in *Arabidopsis*. *New Phytologist* 179:1004−16

45. Li H, Liu Z, Wang X, Han Y, You C, et al. 2023. E3 ubiquitin ligases SINA4 and SINA11 regulate anthocyanin biosynthesis by targeting the IAA29-ARF5-1-*ERF3* module in apple. *Plant, Cell & Environment* 46: 3902−18